

EMPIRICAL CONSTRAINTS ON TROJAN COMPANIONS AND ORBITAL ECCENTRICITIES IN 25 TRANSITING EXOPLANETARY SYSTEMS

N. MADHUSUDHAN¹ & JOSHUA N. WINN¹

Draft version April 4, 2022

ABSTRACT

We present a search for Trojan companions to 25 transiting exoplanets. We use the technique of Ford & Gaudi, in which a difference is sought between the observed transit time and the transit time that is calculated by fitting a two-body Keplerian orbit to the radial-velocity data. This technique is sensitive to the imbalance of mass at the L4/L5 points of the planet-star orbit. No companions were detected above 2σ confidence. The median 2σ upper limit is $56 M_{\oplus}$, and the most constraining limit is $2.8 M_{\oplus}$ for the case of GJ 436. A similar survey using forthcoming data from the *Kepler* satellite mission, along with the radial-velocity data that will be needed to confirm transit candidates, will be sensitive to 10–50 M_{\oplus} Trojan companions in the habitable zones of their parent stars. As a by-product of this study, we present empirical constraints on the eccentricities of the planetary orbits, including those which have previously been assumed to be circular. The limits on eccentricity are of interest for investigations of tidal circularization and for bounding possible systematic errors in the measured planetary radii and the predicted times of secondary eclipses.

Subject headings: techniques: transit photometry, radial velocities — extra-solar planets, trojans — eccentricity

1. INTRODUCTION

Trojan companions are bodies in a 1:1 mean-motion resonance with a planet, librating around one of the two triangular Lagrange points (L4 and L5) of the planet’s orbit around the star. The archetypal example is the population of Trojan asteroids in resonance with Jupiter. Trojan companions to Neptune and Mars have also been detected (Sheppard and Trujillo 2006, Rivkin et al. 2007). Another interesting example is the pair of Saturnian satellites Calypso and Telesto, which are in 1:1 resonance with their fellow satellite Tethys (Reitsema 1981). The presence of Trojan companions and their orbital and physical characteristics have been considered as clues to processes in planet formation and migration. Several recent studies have examined the capture and survival of Trojans in the context of suspected changes in the orbital architecture of the Solar system (Morbidelli et al. 2005, Chiang and Lithwick 2005, Kortenkamp et al. 2004).

Although the Trojan-to-planet mass ratios in the Solar system are very small ($m_T/m_P \sim 10^{-7}$ for Jupiter), it is conceivable that Trojans with much higher mass ratios exist in exoplanetary systems. For circular orbits, even very massive Trojans can be dynamically stable. Laughlin & Chambers (2002) explored the viability of Trojans with mass ratios of unity (i.e., co-orbital planets of equal mass), finding that such configurations can be dynamically stable over time scales comparable to or longer than stellar lifetimes. More generally, the stability of the L4/L5 points depends on the orbital eccentricity and the relative masses of the Trojan, planet, and star (see, e.g., Nauenberg 2002, Dvorak et al. 2004). For many of the known exoplanets, considerations of dynamical stability allow for massive Trojan companions. For example, at least 7 of the known gas giant planets that are within the habitable zones of their parent stars could have dynamically-stable, terrestrial-mass Trojan companions (Schwarz et al. 2007).

Several methods have been proposed to detect Trojan companions to exoplanets. A Trojan may be massive enough to perturb the stellar motion by an amount that is detectable in

the radial-velocity (RV) orbit of the star (Laughlin & Chambers 2002). A Trojan in a nearly edge-on orbit may be large enough for its transit to be detected photometrically (see, e.g., Croll et al. 2007). For a transiting planet, the gravitational perturbations from a Trojan companion may cause a detectable pattern in the recorded transit times (Ford & Holman 2007). Alternatively, Ford & Gaudi (2006) proposed comparing the measured transit times with the times that would be expected based only on the RV data and the assumption of a two-body orbit.

An important virtue of the latter technique is that a sensitive search for Trojans can be performed using only the RV and photometric data that are routinely obtained while confirming transit candidates and characterizing the planets. This is in contrast to the first three methods, for which it is generally necessary to gather new and highly specialized data (very precise RVs, continuous space-borne photometry, and a long sequence of precisely-measured transit times, respectively). For example, Ford & Gaudi (2006) and Narita et al. (2007) placed upper limits on Trojan companions of approximately Neptune mass to the transiting planets HD 209458b, HD 149026b and TrES-1b, using data gathered for other purposes.

In this paper, we present a search for Trojan companions to 25 known transiting exoplanetary systems for which suitable data are available, using the method of Ford & Gaudi (2006, hereafter, “FG”). This paper is organized as follows. The method is described in § 2. The compilation and analysis of the data is described in § 3. The results are given in § 4. These results are summarized and discussed in § 5, which also looks ahead to the prospects for a similar search using data from the *Kepler* mission (Borucki et al. 2008).

As will be explained in § 2, the orbital eccentricity of the planet-star orbit affects the interpretation of the data. Hence, a necessary part of our analysis was the determination of the orbital eccentricity for each system, or the justification of the common assumption that the orbit is circular due to tidal effects. These issues are investigated systematically in § 3. Our findings may be of interest independently of our results on Trojan companions, not only because of the connection to the theory of tidal circularization, but also because the orbital ec-

¹ Department of Physics and Kavli Institute for Astrophysics and Space Research, MIT, Cambridge, MA 02139; nmadhu@mit.edu

centricity affects estimates of the planetary radius via transit photometry, as well as the predicted times of planetary occultations (secondary eclipses). We discuss these points in § 5.

2. METHOD

The basic idea of the FG method is to compare the measured transit time with the expected transit time that is calculated by fitting a two-body Keplerian orbit to the RV data. We will denote by t_O the observed transit time, and by t_C the calculated transit time, in which the calculation is based on fitting a two-body Keplerian orbit to the RV data. The presence of a Trojan companion as a third body would cause a timing offset $\Delta t = t_O - t_C$.

This is most easily understood for the case of a planet on a circular orbit. In such a case, if there is no Trojan companion, the force vector on the star points directly at the planet, and the observed transit time t_O coincides with the time t_V when the orbital velocity of the star is in the plane of the sky (i.e., the time corresponding to the null in the RV variation). If instead there is a single Trojan located at L4 or L5 (or librating with a small amplitude), then the force vector on the star does not point directly at the planet; it is displaced in angle toward the Trojan companion, given by $\tan(\phi) \simeq \sqrt{3}\epsilon/(2-\epsilon)$ where, $\epsilon = m_T/(m_P + m_T)$ for a Trojan mass m_T and a planet mass m_P (Ford & Gaudi 2006). As a result, t_O occurs earlier or later than t_V , and the time difference is given by $\Delta t = \pm \phi P/2\pi$. For small values of the Trojan-to-planet mass ratio, the magnitude of $t_O - t_V$ is proportional to m_T , (Ford & Gaudi 2006):

$$\Delta t \simeq \pm 37.5 \min \left(\frac{P}{3 \text{ days}} \right) \left(\frac{m_T}{10 M_\oplus} \right) \left(\frac{0.5 M_{\text{Jup}}}{m_P + m_T} \right). \quad (1)$$

The positive sign corresponds to a mass excess at the L4 point (leading the planet) while the negative sign corresponds to a mass excess at the L5 point (lagging the planet). Thus, given a Δt , the mass excess can be estimated using Eq. (1), assuming small Trojan-to-planet mass ratio.

More generally, the mass excess is given by:

$$m_T = m_P \left(\frac{2 \tan(2\pi \Delta t/P)}{\sqrt{3} - |\tan(2\pi \Delta t/P)|} \right). \quad (2)$$

For an eccentric two-body orbit, the transit time does not generally coincide with the time of null RV variation, and hence in general $t_C \neq t_V$. To first order, $t_C - t_V \approx (e \cos \omega)P/2\pi$, where e is the eccentricity and ω is the argument of pericenter, and hence one may use the statistic $\Delta t = t_O - t_V - (e \cos \omega)P/2\pi$ to search for Trojan companions. This is how the problem was described by FG, although we find it useful to cast the problem more generally as a comparison between t_O and t_C . We emphasize here that t_O depends solely on photometric observations of transits, while t_C depends almost entirely on RV observations.²

Specifically, one calculates t_C by fitting a two-body Keplerian orbit to the RV data and calculating the expected transit time based on the the fitted orbital parameters (see, e.g., Kane et al. 2008). The true anomaly (f) corresponding to the transit time is

$$f = \frac{\pi}{2} - \omega, \quad (3)$$

from which the eccentric anomaly E can be calculated using

$$\tan \frac{E}{2} = \sqrt{\frac{1-e}{1+e}} \tan \frac{f}{2}, \quad (4)$$

² As explained in § 3, the only sense in which t_C depends on photometric data is that we used the photometrically-determined orbital period P when fitting the RV data, to reduce the number of free parameters.

which in turn leads to the mean anomaly M of the transit using Kepler's equation,

$$M = E - e \sin E. \quad (5)$$

Finally, the calculated transit time t_C is obtained from the definition of the mean anomaly, $M = 2\pi(t - t_P)/P$, where t_P is the time of pericenter passage.

Our basic procedure is therefore to determine t_O from published transit ephemerides, calculate t_C by fitting a two-body Keplerian orbit to the available RV data, and calculate $\Delta t = t_O - t_C$. For circular orbits, we use Eq. (2) to determine the Trojan companion mass m_T corresponding to a given value of Δt . For eccentric orbits, the relationship between t_C and m_T is determined using direct numerical integrations of 3-body systems using a Bulirsch-Stoer algorithm (Varadi et al. 1996). In these integrations, we hold fixed P , e , ω , and the stellar mass m_S at the values given in the literature, and select a Trojan mass m_T and planetary mass m_P such that the RV semi-amplitude (Nauenberg 2002)

$$K = \left(\frac{2\pi G}{P} \right)^{1/3} \frac{\sqrt{m_P^2 + m_T^2 + m_P m_T}}{(m_S + m_P + m_T)^{2/3} \sqrt{1-e^2}}, \quad (6)$$

is equal to the observed value. Hence we simulate the case in which the observed RV variation is due to the combined force of a planet and a Trojan, rather than a planet alone, but the RV data alone are insufficiently precise to discern the difference.³ We compute the transit time t_C , repeat the analysis for an increasing sequence of m_T , and fit a polynomial function to the resulting relationship $t_C(m_T) - t_C(0)$. We found a quadratic function, $m_T = a_1 \Delta t + a_2 (\Delta t)^2$, to give a good fit to the results. Taking m_T to be in Earth masses and Δt in minutes, the coefficients (a_1, a_2) are (0.044, -1.17×10^{-5}) for GJ 436b and (6.787, -0.001) for XO-3b. For the cases of HAT-P-2b and HD 17156b, we find that even very low-mass Trojan companions are dynamically unstable, owing to the large orbital eccentricities (see § 4.2). Thus, for those systems, the requirement of dynamical stability is more constraining than the empirical upper limit on m_T based on the FG method. (As will be described in § 4, this also proved to be true for XO-3b based on the current data.)

3. DATA ANALYSIS

The RV data were taken from the available literature on each system. The references are given in Table 1. These data were generally obtained for the purpose of discovering or confirming the planet, although in a few cases the data were obtained for other reasons, such as precisely measuring the orbital eccentricity (Laughlin et al. 2005) or for measuring the Rossiter-McLaughlin effect (Winn et al. 2006). Regarding the latter, the data that were obtained while a transit was in progress were not used, to avoid the needless complication of incorporating the Rossiter-McLaughlin effect into the RV model. However, in those cases the investigators usually gathered additional data outside of the transit which are useful for refining the spectroscopic orbit.

Our RV model for an eccentric Keplerian orbit has $4+N$ free parameters, where N is the number of independent data sets. Those parameters are the projected planet mass ($m_P \sin i$), orbital eccentricity (e), argument of pericenter (ω), calculated time of midtransit (t_C), and a constant additive velocity (γ)

³ We verified that this discernment is indeed impossible, for $m_T/m_P < 0.5$, for the systems with eccentric orbits considered in this paper.

TABLE 1
DESCRIPTION OF DATA

System	N_v^a	Jitter [m s ⁻¹]	σ_v [m s ⁻¹]	K [m s ⁻¹]	$\xi = 1/\sigma_{(m_T/m_P)}$	References
HD 209458	55	1.4	4.9	83.3	77.7	1,2
HD 17156	24,8	3.3,3.4	3.7,6.2	273.4	72.0	47,48,49,50
HAT-P-7	8	6.5	6.7	213.6	55.3	51
HD 189733	16,44	0.0,0.0	12.0,3.0	201.3	40.6	4
TrES-2	11,5	0.0,0.0	7.5,5.8	181.5	32.2	18,19
HAT-P-3	9	5.1	5.8	98.7	31.3	10
HAT-P-4	9	4.4	5.0	80.8	29.6	11
WASP-3	6	0.0	13.8	247.7	26.9	27
WASP-5	11	11.6	21.8	276.4	25.8	29
TrES-3	11	30.0	31.6	370.4	23.8	20
HAT-P-6	13	10.1	11.2	116.2	23.0	13
GJ436	52	3.4	4.2	18.3	19.4	45,46
WASP-4	13	22.3	28.0	240.3	18.9	28
HD 149026	16	5.4	6.1	46.4	18.7	3
HAT-P-2	13,10,7	34.8,88.7,21.4	35.5,104.5,24.7	980.0	16.8	7,8,9
WASP-2	7	16.6	17.7	157.6	14.4	25,26
WASP-1	7,5	2.7,0.0	3.9,13.3	127.8	12.8	22,23,24
XO-3	10,10	0.0,0.0	171.3,159.0	1486.2	12.3	34
HAT-P-1	15,8	4.4,0.0	6.4,7.4	59.0	11.9	5,6
TrES-4	4	0.0	10.8	98.3	11.1	21
TrES-1	7,8,5	0.0,0.0,0.0	12.1,14.6,3.4	112.0	9.7	14,15,16,17
CoRoT-Exo-1	9	34.0	47.5	190.9	7.4	52
CoRoT-Exo-2	8,4,3,9	60.0,60.0,0.0,0.0	68.4,61.7,27.7,19.0	594.4	7.3	53,54
XO-2	9	15.6	25.0	84.1	6.2	33
HAT-P-5	8	33.4	37.7	134.0	6.2	12
OGLE-TR-182	20	29.7	59.5	120.0	5.5	43
OGLE-TR-113	8	83.5	93.1	286.1	5.3	41
OGLE-TR-211	20	23.7	55.4	82.0	4.1	44
OGLE-TR-56	11	89.0	153.1	268.3	3.6	37,38
OGLE-TR-111	8	0.0	40.2	78.0	3.4	39,40
OGLE-TR-132	5	51.0	68.7	167.0	3.3	42
OGLE-TR-10	9	0.0	63.2	80.0	2.3	35,36
XO-1	4,6	0.0,0.0	65.1,16.8	120.1	2.2	30,31,32

REFERENCES. — (1) Laughlin et al. 2005a; (2) Winn et al. 2005; (3) Wolf et al. 2007; (4) Winn et al. 2007a; (5) Bakos et al. 2007a; (6) Winn et al. 2007b; (7) Bakos et al. 2007b; (8) Winn et al. 2007c; (9) Loeillet et al. 2007; (10) Torres et al. 2007a; (11) Kovacs et al. 2007; (12) Bakos et al. 2007c; (13) Noyes et al. 2008; (14) Alonso et al. 2004; (15) Laughlin et al. 2005b; (16) Narita et al. 2007a; (17) Winn et al. 2007d; (18) O’Donovan et al. 2007a; (19) Holman et al. 2007; (20) O’Donovan et al. 2007b; (21) Mandushev et al. 2007; (22) Collier Cameron et al. 2007; (23) Stempels et al. 2007; (24) Charbonneau et al. 2007; (25) Winn et al. 2008; (26) Charbonneau et al. 2007; (27) Pollaco et al. 2007; (28) Wilson et al. 2008; (29) Anderson et al. 2008; (30) McCullough et al. 2006; (31) Holman et al. 2006; (32) Wilson et al. 2006; (33) Burke et al. 2007; (34) Johns-Krull et al. 2007; (35) Konacki et al. 2005; (36) Pont et al. 2007a; (37) Torres et al. 2004; (38) Pont et al. 2007b; (39) Pont et al. 2007c; (40) Winn et al. 2007e; (41) Bouchy et al. 2004; (42) Bouchy et al. 2004; (43) Pont et al. 2007d; (44) Udalski et al. 2008; (45) Maness et al. 2007; (46) Gillon et al. 2007; (47) Fisher et al. 2007; (48) Narita et al. 2007b; (49) Gillon et al. 2007; (50) Irwin et al. 2008; (51) Pal et al. 2008; (52) Barge et al. 2008; (53) Alonso et al. 2008; (54) Bouchy et al. 2008.

^a Multiple values represent multiple data sets available for the system.

for each data set. In practice we use parameters $e \cos \omega$ and $e \sin \omega$ instead of e and ω because for small e , the errors in $e \cos \omega$ and $e \sin \omega$ are uncorrelated (see, e.g., Winn et al. 2005, Shen & Turner 2008). The orbital period P is held fixed at the photometrically determined value, but of course the transit time t_C is not constrained by the photometric data, since it is the difference between t_C and the actual transit time t_O that we are trying to measure. In two cases for which a long-term acceleration has been identified in the RV data (GJ 436b and CoRoT-Exo-1b), we include an additional free parameter, γ^4 . We assign a different γ to each RV data set, to allow for telescope-specific velocity offsets. The stellar masses for the systems were taken from the homogeneous analysis of Torres et al. (2008) when possible, and otherwise from the discovery paper.

3.1. Estimation of Jitter

⁴ For the remaining systems, we have assumed that the acceleration term is zero. Any real acceleration (and any other failures of the single-Keplerian model) will appear as “noise” in our analysis and will be reflected in a larger estimate of stellar “jitter” (see § 3.1). We find that our results for Δt do not depend much on whether or not a long-term acceleration is allowed as an additional parameter, because the error in this parameter is not strongly correlated with the error in Δt .

For each system, we first analyzed the data with the goal of reproducing the quoted results in the literature. We fitted a Keplerian model to the RV data by minimizing the χ^2 statistic using the AMOEBA algorithm (Press et al. 1992). The initial conditions for the free parameters were taken to be the literature values, and for consistency, for this step we used the exact same choices of P and m_S as in the literature. We define χ^2 as

$$\chi^2 = \sum_{i=1}^{N_v} \left(\frac{v_{i,O} - v_{i,C}}{\sigma_i} \right)^2, \quad (7)$$

where $v_{i,O}$ and $v_{i,C}$ are the observed and calculated radial velocities, respectively, and σ_i is the corresponding uncertainty. The uncertainty should include the statistical uncertainty σ_{stat} , as well as the systematic error σ_{sys} due to unmodeled instrumental systematic errors and intrinsic variations of the stellar photosphere, often referred to as “stellar jitter” in this context (Wright 2006). To estimate the appropriate values of σ_i for this project, we determined the value of σ_{sys} such that $\chi^2/N_{\text{dof}} = 1$ when using

$$\sigma_i = \sqrt{\sigma_{\text{stat}}^2 + \sigma_{\text{sys}}^2} \quad (8)$$

in Eq. (7). Our estimates of the stellar jitter using this procedure are given in Table 1.

3.2. Data Selection

Our desire was to perform as wide a search as possible, using all publicly available data, but for some systems the RV data is so sparse that meaningful constraints cannot yet be obtained. To guide our selection of systems, we used a figure-of-merit based on the results of the Fisher information analysis presented by FG. Those authors showed that in the limit of continuous RV sampling with uniform errors, the uncertainty in Δt will approach $\sigma_{\Delta t} = (1/2\pi^2 N_v)^{1/2} P \sigma_v / K$, where N_v is the number of radial-velocity data points and σ_v is the error per point. For a circular orbit the corresponding uncertainty in m_T will approach $\sigma_{m_T} = (8/3N_v)^{1/2} m_p \sigma_v / K$. Thus, it is possible to estimate the expected uncertainty in Δt and m_T , given the published system parameters, without fitting the actual data. We calculated the figure of merit

$$\xi \equiv \frac{\sqrt{(3N_v/8)K}}{\sigma_v} \approx 1/\sigma_{(m_T/m_p)} \quad (9)$$

for each system in the literature at the outset of this project, and ranked the systems accordingly. Table 1 shows ξ for all the systems, along with N_v , σ_v , and K . For systems where multiple data sets are available, the effective $\sigma_v/N_v^{1/2}$ is obtained by adding in quadrature the corresponding terms from the different data sets. A higher value of ξ reflects better quality of data. From MCMC analyses of all the systems, we find that for systems with $\xi < 6$, the fitting algorithm is susceptible to poor convergence and allows for unphysical parameter ranges. Since the scientific return on such low- ξ systems is comparatively poor we decided to remove them from consideration rather than eliminate these fitting problems. In what follows we focus exclusively on the 25 systems with $\xi > 6$.

3.3. Assumptions for orbital eccentricity

As explained in § 2, the orbital eccentricity affects the calculation of t_C and also affects the relation between Δt and the possible Trojan companion mass m_T . Hence it is imperative to consider the possibility of eccentric orbits. Most of the currently known transiting planets are in very close orbits, where the effects of tidal interactions between the star and planet—and orbital circularization in particular—are expected to be significant (Rasio et al. 1996, Trilling 2000, Dobbs-Dixon et al. 2004). A common practice is to assume that, in the absence of positive evidence for an eccentric orbit, the orbital eccentricity has been reduced to insignificance by the action of tides.

If the assumption of a circular orbit could be justified, it would be advantageous for the present study because it would remove 2 free parameters from the Keplerian model (e and ω) and thereby strengthen the determination of the other parameters, including the key parameter t_C . Our approach was to assume the orbit to be circular only when (1) a circular orbit is consistent with the RV data, (2) the estimated stellar age is more than 20 times larger than the estimated timescale for tidal circularization, and (3) no constraint on $e \cos \omega$ is available because no planetary occultations (secondary eclipses) have been observed. These points are explained in detail in the paragraphs to follow.

To test whether the RV data are consistent with a circular orbit, we fitted a Keplerian model to the RV data using

a Markov Chain Monte Carlo (MCMC) technique, employing a Metropolis-Hastings algorithm within the Gibbs sampler (see, e.g., Tegmark et al. 2004; Ford 2005; Holman et al. 2006; Winn et al. 2007a). For this step, the free parameters were $m_p \sin i$, $e \cos \omega$, $e \sin \omega$ and a γ for each data set. Uniform priors were used for all parameters. The fitting statistic, χ^2 , was defined in Eq. (7). A single chain of $\sim 10^6$ links was used for each system. The jump sizes for the various parameters were set such that the acceptance rate for each parameter was $\sim 20\%$. For each parameter, we found the mode of the *a posteriori* distribution (marginalized over all other parameters), and the 68.3% confidence interval, defined as the range that excludes 15.9% of the probability at each extreme of the *a posteriori* distribution. For cases when $e \cos \omega$ and $e \sin \omega$ were both consistent with zero, we also found the 95.4%-confidence upper limit on e . Table 2 gives the results. All of the systems were found to be consistent with a circular orbit, except for the 4 well-known eccentric systems GJ 436, HAT-P-2, HD 17156, and XO-3.

For the estimated timescale for tidal circularization, we used (Goldreich & Soter 1966):

$$\tau_{\text{circ}} = \frac{4}{63} Q \left(\frac{a^3}{G m_S} \right)^{1/2} \frac{m_p}{m_S} \left(\frac{a}{R_p} \right)^5, \quad (10)$$

which is based on the highly simplified, widely-used model of tidal dissipation in which the tidal bulge experiences a constant phase lag due to tidal friction. Here, a is the orbital separation, and R_p is the radius of the planet. The dimensionless number Q is inversely proportional to the dissipation rate. In the solar system, Jupiter is thought to have $Q \sim 10^5$ (Ioannou & Lindzen 1993) to the extent that this simplified model is applicable. For our purpose, a necessary condition for assuming the orbit to be circular was that $\tau_{\text{star}}/\tau_{\text{circ}} > 20$, i.e., there have been at least 20 e -foldings of tidal circularization, according to this model. In calculating τ_{circ} we assumed $Q = 10^6$, which is conservative in the sense that a larger Q corresponds to a longer calculated timescale for circularization, and a smaller risk that we are assuming a circular orbit when this assumption is not justified.

For a few systems, additional constraints on the orbital eccentricity are available because a planetary occultation (secondary eclipse) has been observed. For small eccentricities, the variables $e \cos \omega$ and $e \sin \omega$ are directly related to the interval between the transit and occultation, and the relative durations of those two events (Kallrath & Milone 1999, Charbonneau et al. 2005):

$$e \cos \omega = \frac{\pi}{2P} \left(t_{\text{occ}} - t_{\text{tra}} - \frac{P}{2} \right), \quad (11)$$

$$e \sin \omega = \frac{\Theta_{\text{tra}} - \Theta_{\text{occ}}}{\Theta_{\text{tra}} + \Theta_{\text{occ}}} \quad (12)$$

where t_{tra} and t_{occ} are the times of transit and occultation, and Θ_{tra} and Θ_{occ} are the corresponding durations. In all cases to date, the bounds on $e \sin \omega$ that follow from this relation are weaker than bounds from the RV data (see, e.g., Winn et al. 2005), and the bounds on $e \cos \omega$ are more constraining. Thus, for those cases in which an occultation has been observed, we add a term to our χ^2 statistic to enforce the corresponding constraint on $e \cos \omega$:

$$\chi^2 = \sum_{n=1}^{N_v} \left(\frac{v_O - v_C}{\sigma_v} \right)^2 + \left(\frac{(e \cos \omega)_O - (e \cos \omega)_C}{\sigma_{e \cos \omega}} \right)^2, \quad (13)$$

TABLE 2
INFERRED ORBITAL ECCENTRICITIES AND RELATED PARAMETERS

System	$e \cos \omega$	$e \sin \omega$	e^a	τ_* ^b	τ_{circ} ^c	$\tau_*/\tau_{\text{circ}}$
CoRoT-Exo-1	+0.011 ^{+0.038} _{-0.071}	-0.073 ^{+0.133} _{-0.135}	< 0.284	8.00	0.00	3179.24
CoRoT-Exo-2	-0.009 ^{+0.020} _{-0.025}	+0.054 ^{+0.025} _{-0.027}	< 0.101	0.50	0.02	29.86
GJ 436	+0.134 ^{+0.006} _{-0.006}	-0.016 ^{+0.045} _{-0.007}	0.138 ^{+0.013} _{-0.007}	6.00	1.15	5.23
HAT-P-1	+0.009 ^{+0.021} _{-0.029}	+0.008 ^{+0.048} _{-0.049}	< 0.099	2.70	0.37	7.30
HAT-P-2	-0.516 ^{+0.005} _{-0.006}	-0.059 ^{+0.014} _{-0.016}	0.520 ^{+0.004} _{-0.005}	2.60	57.59	0.05
HAT-P-3	+0.023 ^{+0.053} _{-0.053}	+0.033 ^{+0.062} _{-0.103}	< 0.194	1.50	0.31	4.78
HAT-P-4	-0.013 ^{+0.026} _{-0.014}	-0.054 ^{+0.054} _{-0.040}	< 0.123	4.60	0.09	50.18
HAT-P-5	+0.026 ^{+0.095} _{-0.095}	-0.039 ^{+0.105} _{-0.228}	< 0.442	2.60	0.09	27.98
HAT-P-6	+0.003 ^{+0.016} _{-0.023}	+0.042 ^{+0.054} _{-0.034}	< 0.101	2.30	0.32	7.26
HAT-P-7	-0.006 ^{+0.012} _{-0.013}	+0.000 ^{+0.016} _{-0.019}	< 0.038	2.20	0.05	47.88
HD 149026	-0.001 ^{+0.001} _{-0.001}	+0.109 ^{+0.042} _{-0.068}	< 0.179	1.90	1.10	1.73
HD 17156	-0.348 ^{+0.009} _{-0.011}	+0.573 ^{+0.006} _{-0.006}	0.669 ^{+0.008} _{-0.007}	5.70	2152.22	0.00
HD 189733	+0.001 ^{+0.000} _{-0.000}	-0.005 ^{+0.012} _{-0.011}	< 0.024	6.80	0.05	136.62
HD 209458	+0.001 ^{+0.002} _{-0.002}	+0.008 ^{+0.011} _{-0.014}	< 0.028	3.10	0.11	27.22
OGLE-TR-10	+0.245 ^{+0.429} _{-0.886}	+0.436 ^{+0.357} _{-0.264}	< 1.000	3.20	0.13	25.54
OGLE-TR-111	+0.163 ^{+0.616} _{-0.028}	+0.099 ^{+0.072} _{-0.559}	< 0.964	8.80	0.51	17.39
OGLE-TR-113	-0.044 ^{+0.092} _{-0.087}	+0.152 ^{+0.104} _{-0.187}	< 0.417	13.20	0.01	1204.61
OGLE-TR-132	+0.247 ^{+0.529} _{-0.198}	+0.279 ^{+0.084} _{-0.477}	< 0.993	1.20	0.02	72.76
OGLE-TR-182	-0.071 ^{+0.064} _{-0.448}	+0.352 ^{+0.147} _{-0.213}	< 0.960	2.00	0.83	2.41
OGLE-TR-211	+0.007 ^{+0.150} _{-0.170}	+0.144 ^{+0.244} _{-0.244}	< 0.858	2.00	0.15	12.91
OGLE-TR-56	+0.003 ^{+0.279} _{-0.790}	+0.519 ^{+0.251} _{-0.399}	< 0.998	3.20	0.00	1139.56
TRES-1	+0.003 ^{+0.002} _{-0.002}	-0.039 ^{+0.030} _{-0.028}	< 0.084	3.70	0.19	19.75
TRES-2	+0.022 ^{+0.015} _{-0.017}	-0.024 ^{+0.019} _{-0.027}	< 0.078	5.00	0.07	75.20
TRES-3	+0.028 ^{+0.016} _{-0.018}	-0.031 ^{+0.036} _{-0.040}	< 0.101	0.60	0.00	137.03
TRES-4	+0.199 ^{+0.056} _{-0.642}	+0.434 ^{+0.054} _{-0.590}	< 0.859	2.90	0.05	54.60
WASP-1	+0.006 ^{+0.031} _{-0.038}	+0.009 ^{+0.035} _{-0.039}	< 0.088	3.00	0.02	129.19
WASP-2	-0.231 ^{+0.331} _{-0.007}	-0.016 ^{+0.058} _{-0.387}	< 0.547	5.60	0.05	116.01
WASP-3	-0.012 ^{+0.027} _{-0.019}	+0.015 ^{+0.047} _{-0.039}	< 0.098	2.10	0.02	93.68
WASP-4	+0.009 ^{+0.021} _{-0.024}	+0.018 ^{+0.047} _{-0.042}	< 0.096	2.00	0.00	931.94
WASP-5	+0.032 ^{+0.017} _{-0.017}	+0.026 ^{+0.027} _{-0.033}	< 0.088	2.00	0.03	77.79
XO-1	+0.017 ^{+0.064} _{-0.149}	+0.066 ^{+0.099} _{-0.191}	< 0.290	1.00	0.43	2.32
XO-2	+0.014 ^{+0.056} _{-0.056}	-0.216 ^{+0.160} _{-0.177}	< 0.515	5.80	0.12	48.43
XO-3	+0.217 ^{+0.016} _{-0.016}	-0.063 ^{+0.034} _{-0.031}	0.229 ^{+0.016} _{-0.018}	2.70	2.98	0.91

^a 95.4 % confidence limits on eccentricity. For four systems which are clearly eccentric, the mode and the 68.3% confidence limits are reported.

^b Nominal age of the system in Gyr: Taken from Torres et al. 2008, when possible, and from the discovery papers for systems not analyzed by Torres et al. 2008. For Corot-Exo-1, we assume a nominal age of 8 Gyr based on the reasoning that is has to be a fairly old main-sequence star (see Barge et al. 2008).

^c Circularization time-scale (in Gyr) for the planetary orbit, assuming $Q = 10^6$ (see the text).

TABLE 3
CONSTRAINTS ON $e \cos \omega$ FROM SECONDARY ECLIPSE
OBSERVATIONS

System	$e \cos \omega^a$	Reference ^b
HD 209458	0.0002 ± 0.0021	Deming et al. 2005
HD 189733	0.0012 ± 0.0002	Knutson et al. 2007
HD 149026	-0.0011 ± 0.0009	Harrington et al. 2007
TrES-1	0.0030 ± 0.0019	Charbonneau et al. 2005
GJ 436	0.1346 ± 0.0059	Deming et al. 2007

^a Evaluated from the transit ephemeris and the secondary eclipse time using Eqn. (11).

^b Reference in literature from which the secondary eclipse time was obtained.

where $(e \cos \omega)_o$ and $(e \cos \omega)_c$ are the ‘‘observed’’ and calculated values of $e \cos \omega$. By ‘‘observed’’ we mean the value that follows from the measured interval between transits and occultations when inserted into Eq. (11). The 5 systems in this category, and the constraints on $e \cos \omega$, are listed in Table 3. In those cases, because such a powerful empirical constraint is available, we do not assume the orbit to be circular even if the RV data are consistent with a circular orbit and $\tau_*/\tau_{\text{circ}} > 20$.

3.4. Constraints on the masses of Trojan companions

For each system, after determining the appropriate level of stellar jitter and deciding whether or not the assumption of a circular orbit is justified, we determined the key parameter t_C and its uncertainty using the same MCMC code that was described in the previous section. In all cases the free parameters included $m_P \sin i$, γ , and t_C . In cases for which the a circular orbit was not assumed, we also fitted for $e \cos \omega$ and $e \sin \omega$. For the special cases of GJ 436 and CoRoT-Exo-1, a velocity gradient $\dot{\gamma}$ was also included as a free parameter. The basic fitting statistic, χ^2 , was defined in Eq. (7), and for the systems in Table 3 an *a priori* constraint on $e \cos \omega$ was applied as in Eq. (13).

To determine the photometric transit time t_O , we used the most precise published photometric ephemeris to compute a predicted transit time close to the midpoint of the RV time series. We then computed the key parameter $\Delta t = t_O - t_C$, the difference between the photometrically observed transit time and the transit time calculated from the RV data assuming zero Trojan mass. In all cases, the uncertainty in t_O is negligible in comparison to the uncertainty in t_C . The results for Δt are translated into constraints on the Trojan mass m_T using Eq. (2) for circular orbits, and using the numerical inte-

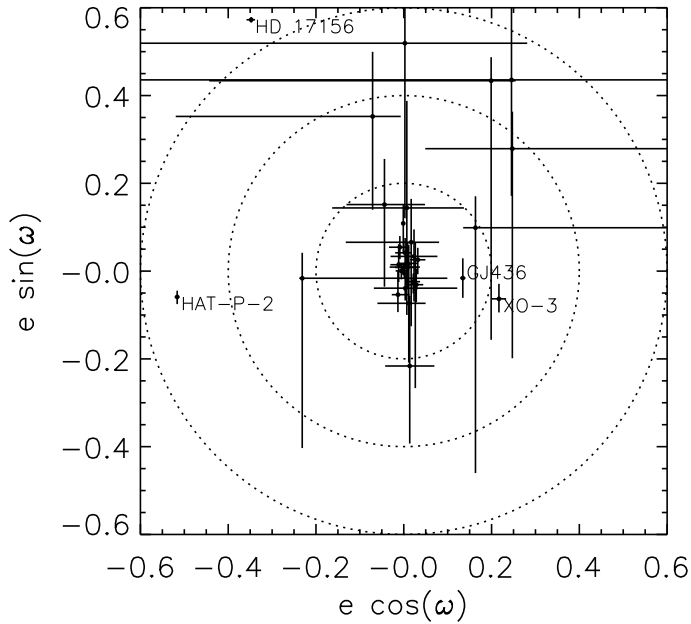


FIG. 1.— Constraints on $e \cos \omega$ and $e \sin \omega$ based on fitting a Keplerian orbit to the RV data, and using constraints from the observed time of the secondary eclipse when available. The four clearly eccentric systems are labeled. The dotted circles show the eccentricity contours corresponding to $e = 0.2, 0.4$ and 0.6 .

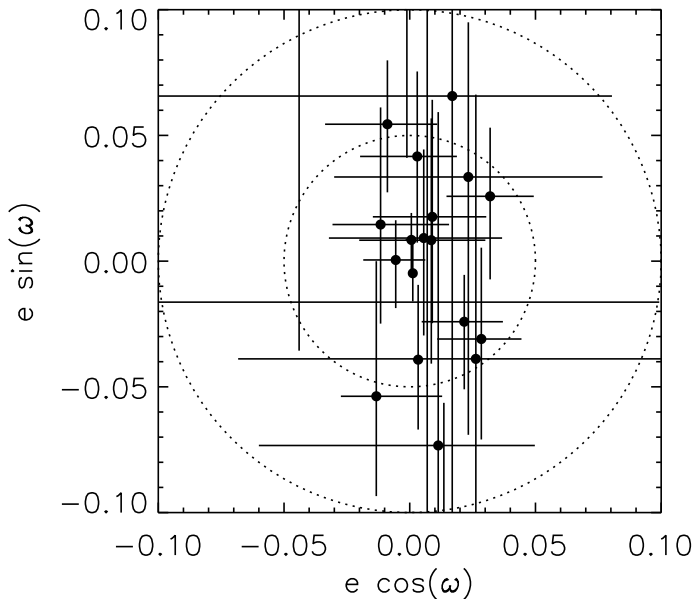


FIG. 2.— The inner region of Fig 1. The dotted circles show the eccentricity contours corresponding to $e = 0.05$ and 0.1 .

grations described in § 2 for eccentric orbits.

4. RESULTS

4.1. Constraints on Trojan Masses

Table 4 gives the 68.3% (1σ) confidence intervals for Δt and m_T for all 25 systems under consideration, as well as the

95.4% (2σ) upper limits on m_T and m_T/m_P . In all the cases, the result for Δt was consistent with zero within 2σ . The system that was closest to a 2σ detection was WASP-2, for which $\Delta t = -123^{+64}_{-53}$ minutes. The result for WASP-2 is therefore worth following up with additional RV data. However, in a sample of 25 systems, even if Δt is always consistent with zero, one expects approximately one 2σ outlier. Hence our survey has not produced compelling evidence for a Trojan companion in this ensemble.

The 2σ upper limits on m_T and on m_T/m_P are shown in Figures 3 and 4, respectively. The systems are ordered from least-constrained to best-constrained, going from left to right. The median upper limit on m_T is $56 M_\oplus$, with the most constraining limit of $2.8 M_\oplus$ holding for the Neptune-sized planet GJ 436. Such a powerful upper limit is possible in this case because of the small stellar and planetary masses, and the copious RV data that is available for this system. The median upper limit on the mass ratio m_T/m_P is 0.1.

It is possible to compare our results to those obtained previously for 3 particular systems. For HD 209458, FG found $\Delta t = 13 \pm 9$ minutes and we find 2^{+11}_{-9} min. For HD 149026, FG found $\Delta t = -13 \pm 27$ min and we find 26^{+29}_{-38} min. For TrES-1, Narita et al. (2007) found $\Delta t = -3.2 \pm 11.8$ min, assuming a circular orbit, and we find -4^{+13}_{-11} min, allowing the orbit to be eccentric but using the constraint on $e \cos \omega$ from secondary eclipse. These results are all consistent with zero with approximately the same range of uncertainty. Minor differences in the quoted central values are probably attributable to minor differences in the fitting procedures and in reporting median values of the *a posteriori* distributions rather than modes. We also find our uncertainties to be in general agreement with the forecasted uncertainties based on the Fisher information analysis of FG.

4.2. Considerations of dynamical stability

For a planet on a circular orbit, non-librating Trojan companions are stable as long as the masses satisfy the condition (Laughlin & Chambers 2002):

$$\frac{m_P + m_T}{(m_S + m_P + m_T)} \leq 0.03812, \quad (14)$$

where m_S , m_P and m_T are the masses of the star, planet and Trojan companion, respectively. This criterion allows for Trojan “companions” that are just as massive as the planet itself, even for planets as massive as $10 M_{\text{Jup}}$ around a Sun-like star.

However, the condition for stability of Trojan companions depends strongly on the eccentricity of the orbit. Nauenberg (2002) reported just such a study, showing the stability domain of bodies in 1:1 resonance as a function of the eccentricity of the orbit and the Routh parameter (γ_R) given by:

$$\gamma_R = \frac{m_S m_P + m_P m_T + m_S m_T}{(m_S + m_P + m_T)^2}. \quad (15)$$

Given the masses of the three bodies, and the eccentricity of the system, one can calculate γ_R and determine from Fig. 5 of Nauenberg (2002) whether or not the system is stable in 1:1 resonance. Conversely, given the eccentricity of the system, Fig. 5 of Nauenberg (2002) gives the the maximum γ_R allowed for stability which, along with m_S and m_P , gives the maximum Trojan mass allowed in the system.

We calculated such limits on the Trojan masses in the four eccentric systems that we analyzed in this work. We find the mass limits to be zero for HAT-P-2b and HD 17156b (in agreement with the results of our 3-body integrations that

TABLE 4
 OBSERVATIONAL CONSTRAINTS ON TROJAN MASSES

System	Δt [min]	m_T [M_\oplus]	Upper bound (95.4 % confidence)	
			m_T/M_\oplus	m_T/m_p
CoRoT-Exo-1	+0020.6 ^{+0042.2} _{-0042.2}	+0018.0 ^{+0061.4} _{-0042.1}	< 0116.5	< 0.35
CoRoT-Exo-2	+0012.8 ^{+0020.5} _{-0015.7}	+0039.6 ^{+0078.0} _{-0048.0}	< 0153.0	< 0.14
GJ 436	-0005.5 ^{+0034.1} _{-0031.0}	-0000.4 ^{+0001.8} _{-0001.2}	< 0002.8	< 0.12
HAT-P-1	+0126.2 ^{+0069.6} _{-0082.7}	+0022.1 ^{+0021.0} _{-0014.3}	< 0052.9	< 0.32
HAT-P-2	-0055.0 ^{+0031.7} _{-0091.7}	-0146.4 ^{+0086.9} _{-0079.0}	< 0280.5 ^a	< 0.10
HAT-P-3	-0139.2 ^{+0138.3} _{-0100.6}	-0045.7 ^{+0046.4} _{-0097.9}	< 0262.8	< 1.25
HAT-P-4	-0012.5 ^{+0024.4} _{-0018.3}	-0004.4 ^{+0008.2} _{-0007.3}	< 0016.5	< 0.08
HAT-P-5	-0025.5 ^{+0098.6} _{-0108.6}	-0011.8 ^{+0057.1} _{-0072.1}	< 0147.7	< 0.46
HAT-P-6	-0037.0 ^{+0141.3} _{-0171.0}	-0012.6 ^{+0067.9} _{-0097.0}	< 0198.9	< 0.59
HAT-P-7	-0000.6 ^{+0028.6} _{-0009.5}	-0000.8 ^{+0014.2} _{-0012.9}	< 0026.5	< 0.05
HD 149026	+0026.0 ^{+0038.1} _{-0038.1}	+0004.7 ^{+0006.6} _{-0006.6}	< 0016.6	< 0.14
HD 17156	-0018.4 ^{+0093.5} _{-0084.6}	-0004.8 ^{+0024.6} _{-0020.3}	< 0043.8 ^a	< 0.04
HD 189733	-0008.8 ^{+0010.7} _{-0010.7}	-0007.7 ^{+0009.4} _{-0008.8}	< 0022.1	< 0.06
HD 209458	+0002.3 ^{+0012.5} _{-0009.3}	+0000.6 ^{+0008.8} _{-0002.7}	< 0006.1	< 0.03
TrES-1	-0004.4 ^{+0012.7} _{-0011.2}	-0001.6 ^{+0004.6} _{-0004.6}	< 0009.9	< 0.04
TrES-2	-0008.6 ^{+0015.2} _{-0010.6}	-0006.2 ^{+0010.6} _{-0010.6}	< 0024.8	< 0.06
TrES-3	-0014.4 ^{+0010.6} _{-0011.7}	-0034.1 ^{+0025.8} _{-0028.4}	< 0081.3	< 0.14
TrES-4	-0125.0 ^{+0089.0} _{-0080.9}	-0049.3 ^{+0035.4} _{-0037.5}	< 0143.8	< 0.49
WASP-1	-0017.6 ^{+0054.5} _{-0049.5}	-0007.8 ^{+0031.1} _{-0034.4}	< 0070.5	< 0.24
WASP-2	-0122.9 ^{+0063.8} _{-0052.7}	-0082.0 ^{+0042.1} _{-0070.1}	< 0199.1	< 0.74
WASP-3	+0016.1 ^{+0011.7} _{-0012.9}	+0023.8 ^{+0019.3} _{-0017.0}	< 0056.1	< 0.10
WASP-4	-0004.7 ^{+0014.9} _{-0013.2}	-0006.5 ^{+0020.0} _{-0020.0}	< 0043.0	< 0.11
WASP-5	-0014.1 ^{+0012.6} _{-0011.4}	-0021.4 ^{+0019.5} _{-0019.5}	< 0054.7	< 0.11
XO-2	+0034.8 ^{+0100.7} _{-0091.5}	+0009.4 ^{+0047.0} _{-0027.4}	< 0088.2	< 0.49
XO-3	-0057.9 ^{+0068.8} _{-0067.2}	-0384.4 ^{+0479.6} _{-0424.3}	< 1097.6 ^a	< 0.26

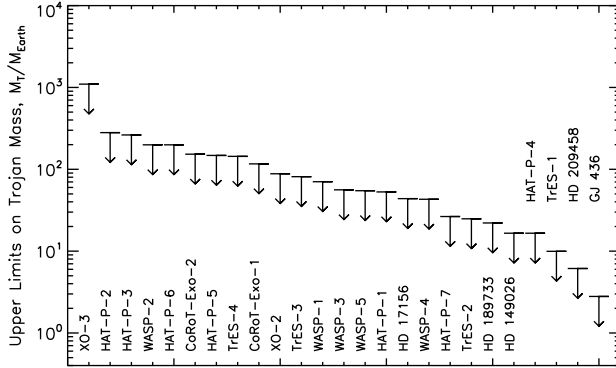
^a For this system the upper limit due to dynamical stability is more constraining than that obtained from the data analysis in this paper using the FG method. Dynamical stability constraints do not allow for Trojan companions to HAT-P-2b and HD 17156b. And, for XO-3b, the upper limit due to stability is 105 M_\oplus .


FIG. 3. — 95.4%-confidence upper limits on masses of Trojan companions. The systems are ordered from the weakest to the strongest upper bound, from left to right.

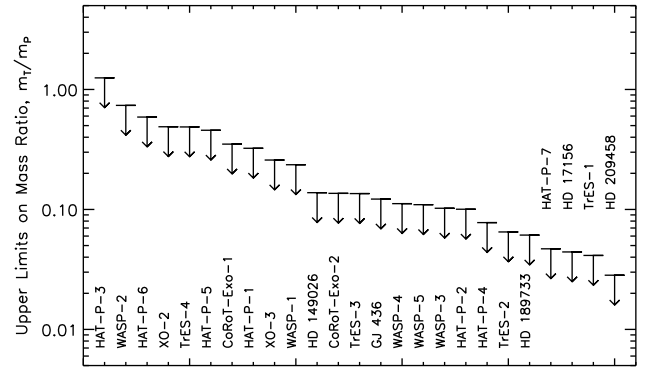


FIG. 4. — 95.4%-confidence upper limits on Trojan-to-planet mass ratios. The systems are ordered from the weakest to the strongest upper bound, from left to right.

were described in § 2), 105 M_\oplus for XO-3b, and 3030 M_\oplus for GJ 436b. Thus, for HAT-P-2b, HD 17156b, and XO-3b, the upper limit on m_T based on considerations of dynamical stability is more constraining than the empirical upper limit using the FG method. For GJ 436b, the upper limit on m_T using the FG method (2.8 M_\oplus) is much stronger than the upper limit imposed by the stability requirement.

5. DISCUSSION

Exoplanetary science has provided enough surprises that an appropriate maxim for observers is: If you can look for a

novel effect or phenomenon that is at least physically plausible, then you should do so, especially when this can be done with existing data. We have obeyed this maxim by conducting a search for Trojan companions to 25 transiting planets. Specifically we have put the technique of FG into practice with a much larger ensemble than has been previously analyzed. We have conducted a search for planets in particular locations (L4/L5) with a median sensitivity of $\sim 56 M_\oplus$, without gathering any new data. Instead, we asked the RV data: when should the transit occur if there is no Trojan companion? Then we consulted the photometric ephemeris to determine when a

transit actually did occur, and interpreted the time difference as a measurement or constraint on Trojan companions. Our results must be understood as constraints on the imbalance of mass residing at the L4 and L5 positions. Equally massive Trojan companions at those positions would produce opposite effects, and no net FG signal, when averaged over the libration periods.

For some systems such as HAT-P-3 and WASP-2, the existing RV data are sparse and noisy enough to allow only the barest constraints on Trojan companions, with masses comparable to the planetary mass. These constraints are nevertheless physically meaningful, in the sense that Laughlin & Chambers (2002) have shown that equal-mass planets in a 1:1 mean-motion resonance and circular orbits can be dynamically stable. In one case, WASP-2, we found a near -2σ evidence for a timing offset that could be interpreted as a Trojan companion. This is not compelling evidence, especially given that we examined a total of 25 systems, but this system is worthy of follow-up. In one case, GJ 436, we have found a 2σ upper limit of $2.8 M_{\oplus}$ on m_T . A positive detection at this level would have represented the least-massive planet detection to date, which is remarkable considering that we did not gather any new data. In no case was there evidence for a timing offset at the 2σ level.

As explained in § 3.3, as part of this study we assessed the justification for assuming that a given planetary orbit is circular, given the existing RV data and reasonable estimates of the stellar age and the timescale for tidal circularization. One part of this assessment was the determination of empirical constraints on $e\cos\omega$ and $e\sin\omega$ based on the RV data. These results may be interesting to other investigators, independently of our results on Trojan companions. The compilation in Table 2 of the results for τ_* and τ_{circ} may be useful to those who are interested in making inferences about the tidal circularization process from the ensemble of transiting planets (see, e.g., Rasio et al. 1996, Trilling 2000, Dobbs-Dixon et al. 2004, Jackson et al. 2008, Mazeh 2008). The limits on $e\cos\omega$ are also useful for bounding the possible error in the predicted times of occultations (secondary eclipses), using the relationship given in Eqn. (11). In addition, although the planetary radius that is determined from transit photometry depends mainly on the observed transit depth, there is a secondary dependence on the transit timescales (the total duration, and the duration of ingress or egress) and the sky-projected orbital speed of the planet during the transit. The latter quantity is not directly observable; it depends on the orbital period, the stellar mass, and the orbital eccentricity and argument of pericenter. Thus there is a secondary dependence of the inferred planetary radius on e and ω (see, e.g., Barnes 2007, or McCullough et al. 2008 for a particular example). The results of Table 2 can be used to bound the systematic error that could arise from this effect.

Having completed this survey using the existing transit data, one may wonder about the achievable limits on Trojan companions using data from ambitious future transit surveys. We consider here the particular case of the *Kepler* satellite mission (Borucki et al. 2008), whose primary goal is the detection of Earth-like planets in the habitable zones of Sun-like stars. *Kepler* is also likely to find larger planets such as gas giants in the habitable zones of their parent stars, and such planets may have lower-mass Trojan companions that are perhaps “more habitable” than the gas giants. Such companions might be detectable photometrically if they are very nearly coplanar with the transiting planet. However, even if they do

not transit, they can be detected with the FG method. It is therefore natural to ask what constraints on Trojan companions will be possible for a given planet that *Kepler* detects in the habitable zone of a Sun-like star, using only the photometric data and the RV data that are routinely gathered for the purposes of confirming and characterizing transiting planets.

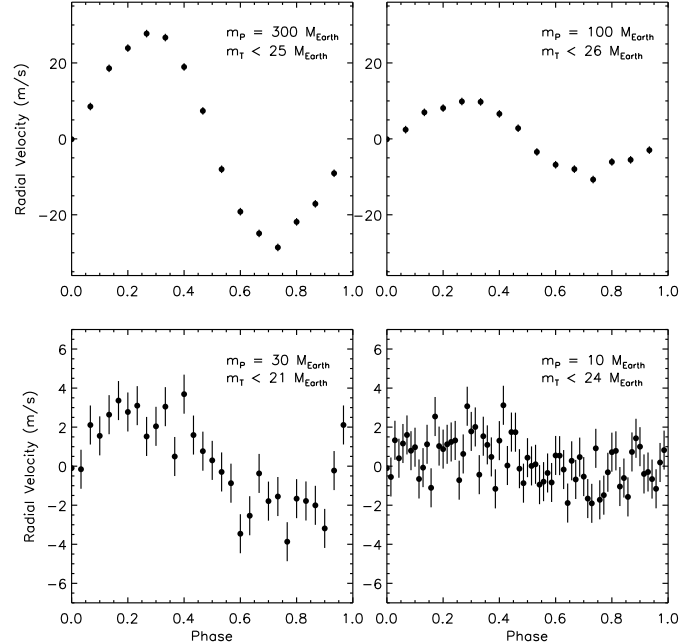


FIG. 5.— Simulated radial velocities and the corresponding 2σ upper limits on Trojan companions to potential *Kepler* detections in the habitable zone around a Sun-like star with $V = 12$.

To answer this question, we consider four different cases, in which *Kepler* finds a planet of mass $300 M_{\oplus}$ (case A), $100 M_{\oplus}$ (B), $30 M_{\oplus}$ (C) or $10 M_{\oplus}$ (D), orbiting a star of solar mass and apparent magnitude $V = 12$, with a period of 1 yr and an orbital eccentricity of 0.1. We simulate RV data for each system with $\sigma_v = 1 \text{ m s}^{-1}$, and a number of data points N_v that seems realistic for the *Kepler* follow-up program. For cases A and B we assume $N_v = 15$. For case C we assume $N_v = 30$, which is sufficient to measure the planetary mass to at least 10% according to the expression for the signal-to-noise ratio from Gaudi & Winn (2007),

$$S/N \simeq 0.6 \left(\frac{m_p}{M_{\oplus}} \right) \left(\frac{N_v}{100} \right)^{1/2} \left(\frac{a}{\text{AU}} \right)^{-1/2} \times \left(\frac{m_s}{M_{\odot}} \right)^{-1/2} 10^{-0.2(V-12)} \frac{D}{3.6 \text{ m}}, \quad (16)$$

which was intended to approximate the case of the HARPS instrument on the ESO 3.6 m telescope. For the challenging case D we assume $N_v = 70$, corresponding to a 20% uncertainty in the planetary mass. We perform a MCMC analysis on the simulated data for each system, just as was done for the 25 transiting systems in this study, and obtain the corresponding constraints on Trojan companion masses.

Fig. 5 shows the simulated data and the results for the four cases. We find the 2σ upper limits on the mass of Trojan companions to be $25 M_{\oplus}$, $26 M_{\oplus}$, $21 M_{\oplus}$, and $24 M_{\oplus}$, for cases A, B, C and D respectively. The results are limited by

the RV follow-up program; the superb photometric precision of *Kepler* does not lead to correspondingly superb constraints on Trojan masses.

The results for cases A–D are all of the same order of magnitude. This is because Trojan detectability depends primarily on $\sigma_v/\sqrt{N_v}$, which only varies by a factor of 2.2 between case A and D. For small m_T/m_P and large ξ (see Eq. 9), Trojan detectability is indeed independent of planet mass for fixed $\sigma_v/\sqrt{N_v}$. A larger planet produces a larger RV semi-amplitude, and hence offers greater sensitivity in measuring Δt , but the conversion from Δt to m_T varies inversely with planetary mass.

However, for cases C and D, this scaling is not precisely obeyed. One reason is that for the larger values of m_T/m_P that are relevant in those cases, the relation between m_T and Δt is nonlinear (see Eq. 2), and therefore the error in m_T is not Gaussian. For case D, there is an additional source of non-Gaussianity: the signal-to-noise ratio is low enough that the correlations between Δt , K , e , and ω become important. This means that the upper limit on m_T is less constraining than one would predict based only on $\sigma_v/\sqrt{N_v}$.

We conclude that a “serendipitous” search for Trojan companions to the habitable-zone planets that will be detected and confirmed as part of the *Kepler* program will be sensitive to planets of approximately Neptunian mass or larger. Of course the sensitivity could be improved by obtaining additional RV data as part of a more focused search effort.

Considering the HARPS spectrograph (Pepe et al. 2002), mounted on the 3.6 m ESO telescope, as a fiducial instrument for precise RV measurements, and assuming the noise to be limited by photon-counting statistics, the measurement uncertainty can be obtained by scaling current results (Lovis et al. 2005, Gaudi & Winn, 2007):

$$\sigma_v = \frac{10^{0.2(V-12)}}{D/3.6\text{ m}} \text{m/s}, \quad (17)$$

where V is the apparent visual magnitude of the star, and D is the aperture of the telescope. Here we have assumed a 60 min exposure and a G-type star.

For small Trojan-to-planet mass ratios, and assuming a circular orbit, one can determine a nominal estimate of the sensitivity of current observational facilities to detect Trojan companions to *Kepler* planets. Under these assumptions, the signal-to-noise ratio $\Delta t/\sigma_{\Delta t}$, for detecting a Trojan companion is given by:

$$S/N \simeq 0.56 \left(\frac{m_T}{M_{\oplus}} \right) \left(\frac{N_v}{100} \right)^{1/2} \left(\frac{a}{\text{AU}} \right)^{-1/2} \times \left(\frac{m_S}{M_{\odot}} \right)^{-1/2} 10^{-0.2(V-12)} \frac{D}{3.6\text{ m}} \quad (18)$$

Let us assume a *Kepler* detection of a Jupiter-mass transiting planet at 1 AU around a sun-like star with $V = 12$, observed with the HARPS instrument. Then, considering 100 observations evenly spaced in orbital phase, a 3σ Trojan detection (i.e. $\Delta t > 3\sigma_{\Delta t}$) can be made, if a Trojan mass imbalance of $m_T \gtrsim 5.36M_{\oplus}$ existed in the orbit. If the planet were orbiting instead at 0.03 AU (a “hot Jupiter” orbit), then a detection would be possible for $m_T \gtrsim 0.93M_{\oplus}$. It would seem that searching for Trojan companions is a promising alternate channel for finding small and potentially habitable bodies in the habitable zones of their parent stars, even if the transiting planets themselves are too massive to be habitable.

We thank Jack Wisdom, Scott Gaudi and Eric Ford for helpful conversations. We further thank Scott Gaudi for providing a detailed and helpful review of the manuscript. We are grateful to the William S. Edgerly Innovation Fund for partial support of this work.

REFERENCES

- Agol, E., Steffen, J., Sari, R., & Clarkson, W. 2005, MNRAS, 359, 567
 Alonso, R., et al. 2004, ApJ, 613, L153
 Alonso, R., et al. 2008, A&A, in press(arXiv:0803.3207)
 Anderson, D., et al. 2008, MNRAS, in press (arXiv:0801.1685)
 Bakos, G. Á., et al. 2007a, ApJ, 656, 552
 Bakos, G. Á., et al. 2007b, ApJ, 670, 826
 Bakos, G. Á., et al. 2007c, ApJ, 671, L173
 Barge, P., et al. 2008, A&A, in press(arXiv:0803.3202)
 Barnes, J. W. 2007, PASP, 119, 986
 Borucki, W., et al. 2008, IAU Symposium, 249, 17
 Bouchy, F., Pepe, F., Queloz, D. 2001, A&A, 374, 733
 Bouchy, F., et al. 2004, A&A, 421, L13
 Bouchy, F., et al. 2008, A&A, in press(arXiv:0803.3209)
 Burke, C. J., et al. 2007, ApJ, 671, 2115
 Charbonneau, D., et al. 2005, ApJ, 626, 523
 Charbonneau, D., et al. 2007, ApJ, 658, 1322
 Chiang, E. I., & Lithwick, Y. 2005, ApJ, 628, 520
 Collier Cameron, A., et al. 2007, MNRAS, 375, 951
 Cresswell, P., & Nelson, R. P. 2006, A&A, 450, 833
 Croll, B., et al. 2007, ApJ, 671, 2129
 Deming, D., Seager, S., Richardson, L. J., & Harrington, J. 2005, Nature, 434, 740
 Deming, D., et al. 2007, ApJ, 667, L199
 Dobbs-Dixon, I., Lin, D. N. C., & Mardling, R. A. 2004, ApJ, 610, 464
 Dvorak, R., Pilat-Lohinger, E., Schwarz, R., & Freistetter, F. 2004, A&A, 426, L37
 Fisher, D. A., et al. 2007, ApJ, 669, 1336F
 Ford, E. B., & Gaudi, B. S. 2006, ApJ, 652, L137
 Ford, E. B., & Holman, M. J. 2007, ApJ, 664, L51
 Ford, E. B. 2005, AJ, 129, 1706
 Ford, E. B., & Rasio, F. A. 2006, ApJ, 638, L45
 Gaudi, S. B., & Winn, J. N. 2007, ApJ, 655, 550
 Gillon, M., et al. 2006, A&A, 459, 249
 Gillon, M., et al. 2007a, A&A, 466, 743
 Gillon, M., et al. 2007b, A&A, 471, L51
 Gillon, M., et al. 2008 (arXiv:0712.2073)
 Harrington, J., Luszcz, S., Seager, S., Deming, D., & Richardson, L. J., 2007, Nature, 447, 691
 Holman, M. J., et al. 2006, ApJ, 652, 1715
 Holman, M. J., et al. 2007, ApJ, 655, 1103
 Holman, M. J., & Murray, N. W. 2005, Science, 307, 1288
 Ioannou, P. J., & Lindzen, R. S. 1993, ApJ, 406, 266
 Irwin, J., et al. 2008, ApJ, in press (arXiv:0801.1496)
 Jackson, B., Greenberg, R., & Barnes, R. 2008, ApJ, 678, 1396
 Johns-Krull, C. M., et al. 2007, ApJ, 677, 657
 Kallrath, J., & Milone, E. F. 1999, Eclipsing Binary Stars, Springer-Verlag New York, Inc.
 Kane, S. R. 2007, MNRAS, 380, 1488
 Knutson, H. A., et al. 2007, Nature, 447, 183
 Konacki, M., Torres, G., Sasselov, D. D., & Jha, S. 2005, ApJ, 624, 372
 Kovács, G., et al. 2007, ApJ, 670, L41
 Laughlin, G., & Chambers, J. E. 2002, AJ, 124, 592
 Laughlin, G., et al. 2005a, ApJ, 629, L121
 Laughlin, G., et al. 2005b, ApJ, 621, 1072
 Li, C.-H., et al. 2008, Nature, 452, 610
 Loeillet, B., et al. 2008, A&A, 481, 529
 Lovis, C., et al. 2005, A&A, 437, 1121
 Maness, H. L., et al. 2007, PASP, 119, 90
 Mandushev, G., et al. 2007, ApJ, 667, L195
 Mazeh, T. 2008, EAS Publications Series, 29, 1
 McCullough, P. R., et al. 2006, ApJ, 648, 1228
 McCullough, P. R., et al. 2008, ArXiv e-prints, 805, arXiv:0805.2921
 Morbidelli, A., Levison, H. F., Tsiganis, K., & Gomes, R. 2005, Nature, 435, 462

- Murray, C. D., & Dermott, S. F. 2000, *Solar System Dynamics*, Cambridge University Press, Cambridge, UK.
- Narita, N., et al. 2007, *Publ. Astron. Soc. Japan*, 59, 763
- Narita, N., Sato, B., Oshima, O., Winn, J. N., 2008, *Publ. Astron. Soc. Japan*, Vol.60, No.2, pp.L1
- Nauenberg, M. 2002, *ApJ*, 124, 2332
- Noyes, R. W., et al. 2008, *ApJ*, 673, L79
- O'Donovan, F. T., et al. 2006, *ApJ*, 651, L61
- O'Donovan, F. T., et al. 2007, *ApJ*, 663, L37
- Pal, A., et al. 2008, *ApJ*, in press (arXiv:0803.0746)
- Pepe, F., et al. 2002, *The Messenger*, ESO, 110, 9
- Pollaco, D., et al. 2008, *MNRAS*, 385, 1576
- Pont, F., et al. 2004, *A&A*, 426, L15
- Pont, F., et al. 2007, *A&A*, 465, 1069
- Pont, F., et al. 2008, submitted to *A&A*(arXiv:0710.5278)
- Press, W. H., Teukolsky, S. A., Vetterling, W. T., Flannery, B. P. 1992, *Numerical Recipes in C* (Cambridge Univ. Press).
- Rasio, F. A., Tout, C. A., Lubow, S. H., & Livio, M. 1996, *ApJ*, 470, 1187
- Rivkin, A. S., et al. 2007, *Icarus*, 192, 434.
- Schwarz, R., Pilat-Lohinger, Dvorak, R., Érdi, B., & Śandor, Z. 2005, *Astrobiology*, 5, 579
- Schwarz, R., Dvorak, R., Šuli, Á., & Érdi, B. 2007, *A&A*, 474, 1023
- Shen, Y., & Turner, E. L. 2008, *ArXiv e-prints*, 806, arXiv:0806.0032
- Sheppard, S. S., & Trujillo, C. A. 2006, *Science*, 313, 511
- Stempels, H. C., et al. 2007, *MNRAS*, 379, 773
- Tegmark, M., et al. 2004, *Phys. Rev. D.*, 69, 103501
- Thommes, E. W. 2005, *ApJ*, 626, 1033
- Torres, G., Konacki, M., Sasselov, D. D., & Jha, S. 2004, *ApJ*, 609, 1071
- Torres, G., et al. 2007, *ApJ*, 666, L121
- Torres, G., Winn, J. N., & Holman, M. J. 2008, *ApJ*, 677, 1324
- Trilling, D. E. 2000, *ApJ*, 537, L61
- Udalski, A., et al. 2008, *A&A*, 482, 299
- Varadi, F., Ghil, M., Newman, W. I., Kaula, W. M., Grazier, K., Goldstein, D., and Lessnick, M. 1996, <http://astrobiology.ucla.edu/varadi/NBI/NBI.html>
- Wilson, D. M., et al. 2006, *PASP*, 118, 1245
- Wilson, D. M., et al. 2008, *ApJ*, 675, L113
- Winn, J. N., et al. 2005, *ApJ*, 631, 1215
- Winn, J. N., et al. 2006, *ApJ*, 653, L69
- Winn, J. N., et al. 2007a, *ApJ*, 133, 1828
- Winn, J. N., et al. 2007b, *AJ*, 134, 1707
- Winn, J. N., et al. 2007c, *ApJ*, 665, L167
- Winn, J. N., et al. 2007d, *ApJ*, 657, 1098
- Winn, J. N., Holman, M. J., & Fuentes, C. I. 2007e, *AJ*, 133, 11
- Winn, J. N., et al. 2008, *ApJ*, 675, 1531
- Wolf, A. S., et al. 2007, *ApJ*, 667, 549
- Wright, J. 2006, *AAS Meeting 209*, 179.04; *Bulletin of the AAS*, 38, 1157
- Wu, Y., & Murray, N. 2003, *ApJ*, 589, 605